JOINT RECONSTRUCTION IN IN-LINE HOLOGRAPHY COMBINING PARAMETRIC AND NON-PARAMETRIC INVERSE APPROACHES: APPLICATION TO FLUID MECHANICS

Anthony Berdeu, Olivier Flasseur, Loïc Denis, Fabien Momey, Méès Loïc, Nathalie Grosjean, Corinne Fournier

JOINT RECONSTRUCTION IN IN-LINE HOLOGRAPHY COMBINING PARAMETRIC AND NON-PARAMETRIC INVERSE APPROACHES: APPLICATION TO FLUID MECHANICS

Berdeu Anthony[1], Flasseur Olivier[1], Denis Loïc[1], Momey Fabien[1], Méès Loïc[2], Grosjean Nathalie[2], Fournier Corinne[1]

[1]Université Lyon, UJM-Saint-Étienne, CNRS, Institut d'Optique Graduate School, Laboratoire Hubert Curien UMR 5516, F-42023, Saint-Étienne, France
[2]Laboratoire de Mécanique des Fluides et d'Acoustique UMR CNRS 5509, École Centrale de Lyon, Université Claude Bernard Lyon 1, INSA Lyon, 69134 Écully Cedex, France

anthony.berdeu@univ-st-etienne.fr, corinne.fournier@univ-st-etienne.fr

KEYWORDS

Inverse problem approach; Mie propagation; Rayleigh-Sommerfeld propagation

ABSTRACT

In-line digital holography is a simple and powerful tool to image absorbing and/or phase objects in numerous fields such as crystallography, biology or fluid mechanics. Nevertheless, this kind of interference imaging technique leads to a loss of the phase of the complex wave front on the sensor. This lack of phase information can be critical in the reconstruction process. Thus, the simplicity of the setup must be balanced by dedicated reconstruction algorithm to retrieve the object from its hologram, such as inverse approaches. In the case of simple objects for which an analytical model of propagation is known, parametric algorithms are very effective. But these approaches fail at reconstructing more complex objects, where non-parametric solutions must be involved. This may lead to a loss in precision or specificity. In this work we propose a new approach combining these two methods to take benefits from their own advantages. The object to reconstruction is split in two subparts. A part is described by a parametric model. The other part of the object is simulated via a non-parametric model. These two parts which interfere are jointly considered in the reconstruction algorithm by alternating parametric and non-parametric procedures. We apply this new technique to evaporating droplets where the high contrast fringes produced by the droplets tend to mask the fringes produced by the plume. With our method, both the droplet and the plume are jointly reconstructed.

I. INTRODUCTION

In-line holography principle was first introduced by Gabor in the late forties [1]. In this kind of microscopy, as schematically presented in Fig.1a, a coherent light source is scattered by the studied sample that produces a secondary diffracted wave. The incident beam and this diffracted wave interfere on the sensor plane which records the resulting intensity. Interferences with a coherent light are sensitive to amplitude changes and phase delays, making this technique particularly adapted to image absorbing and/or dephasing samples. This high sensitivity is nowadays used in numerous fields such as biology [2,3,4,5], fluid mechanics [6,7,8,9], and particles characterization [10,11,12,13].

Nonetheless its simplicity of implementation is counterbalanced by an inherent drawback: a lack of reference arm leading to a loss of the phase information of the wave front on the sensor plane. If simple back-propagation using the solution of the diffraction equations [15] is sometimes still possible, this technique leads to strong artifacts such as twin-images of the sample to retrieve. Thus, dedicated algorithm must me developed to correctly reconstruct the unknown object.

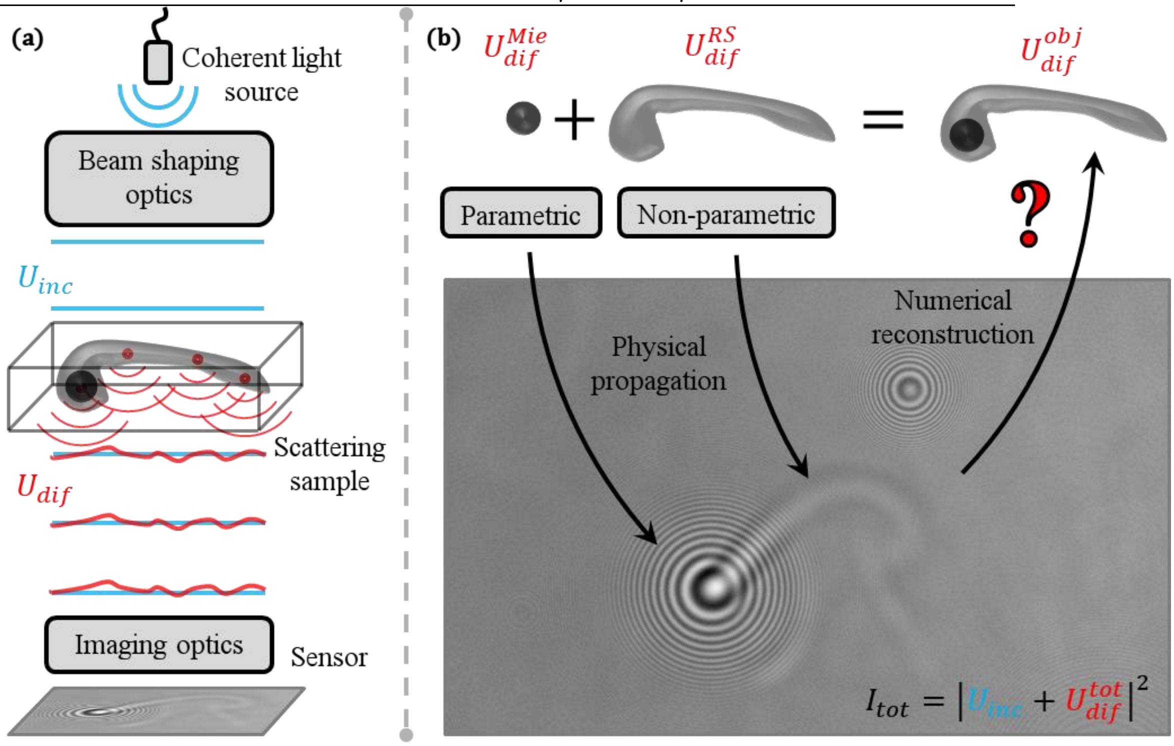

Figure 1: (a) General schematic of in-line holography: a coherent light source produces a coherent incident wavefront U_{inc} that is scattered by the sample, producing a diffracted wavefront U_{dif}. These wavefronts interfere on the sensor plane which records the resulting intensity $I_{tot} = |U_{inc} + U_{dif}|^2$. (b) Schematic of the proposed method in the case of evaporating droplet: the object to reconstruct is composed of two subparts. The wave diffracted by the spherical droplet is given by the Mie model, which is an analytical parametric solution of the diffraction equations. The plume is described by a global non-parametric dephasing plane whose diffracted wave is propagated according to the Rayleigh-Sommerfeld theory. Based on the linearity of the equations of the diffraction, these two subparts interfere to create the total wave diffracted by the object: $U_{dif}^{tot} = U_{dif}^{Mie} + U_{dif}^{obj}$.

First algorithms were mainly based on iterative phase retrieval approach where the unknown is mainly the lost phase on the sensor plane in order to correctly perform the back-propagation [16,17].

Recent techniques takes benefit of inverse problems approach, in which accurate forward models allow reconstruction of the unknown object from the measurements. Two classes of solutions exist.

When the object is simple enough to be described by a few number of parameters, parametric approaches provide robust and highly sensitive techniques to retrieve the sample [6,7,8,10,11,12,13].

When analytical solutions do not exist, reconstruction techniques must shift to non-parametric algorithms in which the object is composed of a high numbers of unknowns, such as the 2D transmittance value [18] or the 3D scattering potential on a sampled grid [5]. Adding physical constraints and wisely chosen regularizations are then necessary to solve the ill-posed problem. Recent works have shown the feasibility to retrieve the lost phase information from single in-line hologram of absorbing and/or phase objects [2,5,9].

In this work, we propose to jointly mix these approaches (Fig.2b), reconstructing the sample by simultaneously using the two techniques. The idea is to use the parametric approach to better constrain the non-parametric unknowns or to reduce their number while injecting more physical constraints in the model. On the other way around, better estimating the surrounding signal that cannot be fitted by the parametric model increases the accuracy of the parameters estimate.

II. PROPOSED METHOD

II.1 General method

The idea is to reconstruct an object x from its experimental in-line intensity hologram I_d, assuming that this object can be decomposed in two subparts x_p and x_{np}. A diffraction model is known for each of this part to predict the diffracted wave U_{dif} on the sensor: a parametric model for x_p and a non-parametric model for x_{np} (see Fig.1b).

From the linearity of the wave equation, the global direct model to simulate the intensity I_s produced by a given object x scattering an incident wave U_{inc} is then:

$$I_s(x_p, x_{np}) = \left|U_{inc} + U_{dif}^{p}(x_p) + U_{dif}^{np}(x_{np})\right|^2$$

This is the principle of the first Born approximation [19]: each part of the sample diffracts a supposed unperturbed incident wave front. Reconstructing x now consists in minimizing the following problem, assuming without loss of generality that $U_{inc} = 1$:

$$\begin{aligned}\tilde{x} = (\tilde{x}_p, \tilde{x}_{np}) &= \underset{x_p, x_{np}, c, o}{\operatorname{argmin}} \left\| res(x_p, x_{np}, c, o) \right\|_W^2 \\ &= \underset{x_p, x_{np}, c, o}{\operatorname{argmin}} \left\| I_d - \left(c. \left|1 + U_{dif}^{p}(x_p) + U_{dif}^{np}(x_{np})\right|^2 + o \right) \right\|_W^2\end{aligned}$$

where res are the residues of the model compared to the experimental data and (c, o) real coefficients to take into account the scaling of the acquisition dynamics and a possible offset in the measurements. W is a matrix of weighting coefficients to possibly take into account the presence of defective pixels [11].

To solve this problem, an iterative hierarchical optimization is implemented, alternating optimization of the parametric model on x_p and optimization of the non-parametric model on (x_{np}, c, o).

II.2 Parametric approach: the Mie model

In the present application in fluid mechanics, the parametric part x_p of the object x are evaporating droplets of ether. Assuming that they are spheres of known refractive index, they can be modeled via the Mie theory [3,20], which provides in the far field regime an analytical solution for the complex scalar field U_{dif}^{Mie}.

The object x_p is described by a limited number of parameters: $x_p = (x, y, z, r)$, the 2D position on the sensor plane, the distance and the radius of each sphere.

For each particle in the field, a first rough estimation is performed using matching pursuit algorithm by browsing the parameters' discretized space with a Thompson model [11,12]. Then, this first estimation is refined with the Mie model, in an iterative inverse approach with a numerical estimation of the gradient at each step.

Thus, at the i_{th} iteration of the alternative approach, once gets:

$$x_p^{i+1} = \underset{x_p}{\operatorname{argmin}} \left\| I_d - \left(c^i. \left|U_{BG}^{np_i} + U_{dif}^{p}(x_p)\right|^2 + o^i \right) \right\|_W^2$$

with the background wave $U_{BG}^{np_i} = 1 + U_{dif}^{np}(x_{np}^i)$.

II.3 Non-parametric approach: the Rayleigh-Sommerfeld propagation

In the present application in fluid mechanics, the non-parametric part x_{np} of the object x are the plumes evaporated by the droplets of ether. Then, the unknown is a 2D map of a complex transmittance t_{2D}, representing the projection of the sample along the line of sight.

The object itself that produces the diffracted wave U_{dif}^{np} is the difference of the transmittance to the unitary plane: $\delta t = t_{2D} - 1$. The resulting diffracted wave at a distance z of this plane is given by the convolution:

$$U_{dif}^{np} = h_{RS}^{\lambda,z}(r) \star \delta t$$

where the convolution kernel $h_{RS}^{\lambda,z}\left(r = \sqrt{x^2 + y^2 + z^2}\right)$ is the Rayleigh-Sommerfeld propagator [5] at the illumination wavelength λ and at the distance z:

$$h_{RS}^{\lambda,z}(r) = \frac{1}{i\lambda}\frac{z}{r}\left(1 - \frac{1}{ikr}\right)\frac{e^{ikr}}{r}$$

In addition, the general problem in describing a complex transmissive plane is to find a practical formulation to split the absorbing and dephasing parts of the object. To do so, t_{2D} is actually modeled by its complex optical length l: $t_{2D} = e^{\frac{2i\pi}{\lambda}l}$. The real part of l consequently gives the dephasing properties of the object and its imaginary part its absorption.

In the present case, the only absorbing objects are the droplets, described by the Mie model. Then, the plumes are only phase objects, having a real optical length. At the i_{th} iteration of the alternative approach, the non-parametric object to reconstruct is consequently this map of real optical length x_{np}:

$$\left(x_{np}^{i+1}, c^{i+1}, o^{i+1}\right) = \underset{x_{np},c,o}{\operatorname{argmin}} \left\| I_d - \left(c.\left| U_{BG}^{p_i} + h_{RS}^{\lambda,z}(r) \star \left(e^{\frac{2i\pi}{\lambda}x_{np}} - 1\right)\right|^2 + o \right) \right\|_W^2$$

with the background wave $U_{BG}^{p_i} = 1 + U_{dif}^{p}\left(x_p^{i+1}\right)$. This problem is solved iteratively by regularizing the term x_{np} while values for (c, o) are analytically computed at each iteration.

III. PRELIMINARY RESULTS

Fig.2 presents the preliminary results of the proposed method on two evaporating droplets. The reconstruction distance z is given by the fit of Mie model for the biggest droplet.

The parametric part of the algorithm (Mie model, Fig.2b,e,h) predicts that the two droplets have a radius of 79.65 and 40.86 microns at a distance of 1.0558 and 0.3876 meter.

The non-parametric part of the algorithm (Rayleigh-Sommerfeld propagation, Fig.2c,f,i) successfully retrieves the evaporated plume as well as the background phase of the flow. Interestingly, it appears that the phase is missing at the droplet position (see medallion in Fig.2b-c), supporting the fact that the droplet behaves as an absorbing particle for the background phase and local plume whose local information is refracted and lost.

By combining the two reconstructed subparts, once gets a global retrieved phase on the sensor plane (Fig.2g). Looking at Fig.2a, it appears that the final error in the residues is below ± 5 %, with the very good agreement in the background, generally hard to reconstruct with standard methods because of the high contrast fringes produced by the droplets.

Fig.2c and its medallion show that the twin-image artifacts present in simple back-propagation is importantly cleaned by the regularization procedure.

IV. CONCLUSION AND DISCUSSION

In this work we provided the proof of concept that a combined parametric and non-parametric approach is feasible on single in-line holograms. The parametric part of the reconstruction effectively fits the high contrast fringes allowing the non-parametric part to subtlety retrieve the faint parts of the object. These reconstructions are jointly performed, meaning that their interferences are rigorously modeled and taken into account, contrary to standard methods which work on subtracted intensities.

Nevertheless some works remain to be done, especially on the non-parametric part of the algorithm. Indeed, even if the background structure is erased in the residues, it appears that for strong intensities such as for the droplet or the concentrated part of the plume some signal remains. It implies that a better choice of regularization and associated hyper-parameters could improve the reconstruction to more quantitative values. Moreover, some twin-image artifacts are still present in the reconstruction.

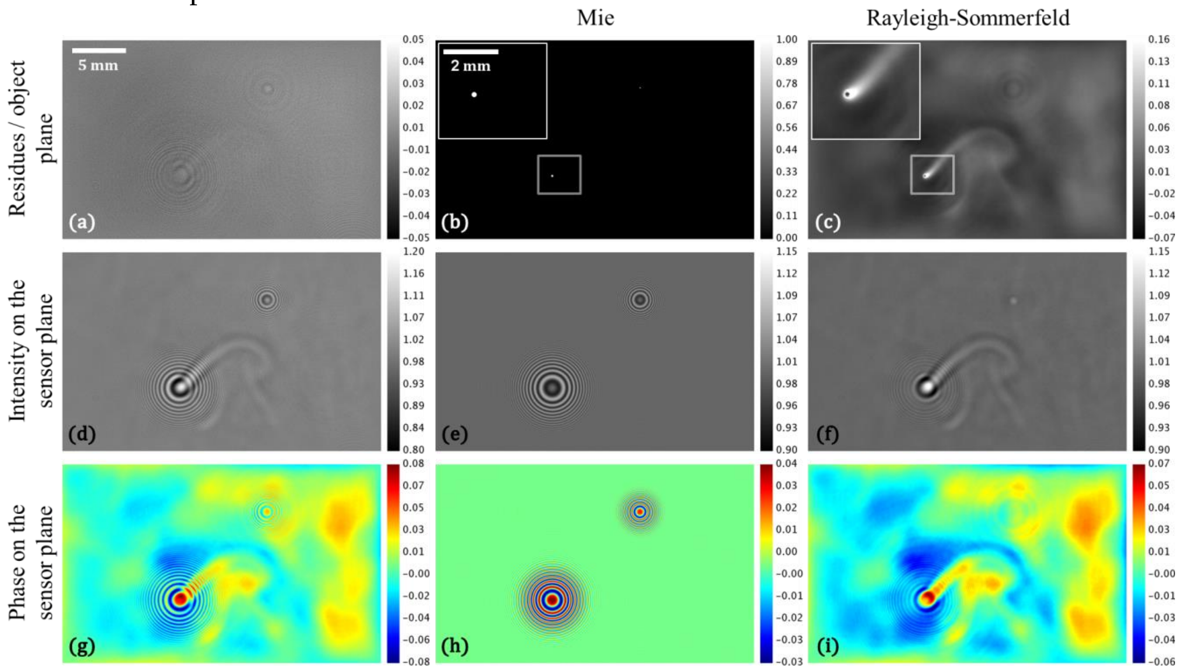

Figure 2: Reconstruction of an in-line hologram of evaporating droplets. (a) Residues of the reconstruction.(b) Reconstruction absorption of the sample given by the Mie model. (c) Reconstructed phase delay induced by the plume and the surrounding flow (radian). (d) Initial raw hologram. (e,h) Intensity and phase (radian) predicted by the Mie part of the model. (f,i) Intensity and phase (radian) predicted by the Rayleigh-Sommerfeld part of the model. (g) Retrieved phase (radian) on the sensor plane.

REFERENCES

[1] D. Gabor (1948) A new microscopic principle, *Nature*, 777–778

[2] Y. Rivenson & al (2016) Sparsity-based multi-height phase recovery in holographic microscopy, *Scientific Reports*, **6**, 37862

[3] E. Mathieu & al (2016) Time-lapse lens-free imaging of cell migration in diverse physical microenvironments, *Lab on a chip*, **16**(17), 3304–3316

[4] C. Allier & al (2017) Imaging of dense cell cultures by multiwavelength lens-free video microscopy, *Cytometry Part A*, **91**(5), 433–442

[5] A. Berdeu & al (2017) Comparative study of fully three-dimensional reconstruction algorithms for lens-free microscopy, *Applied Optics*, **56**, 3939–3951

[6] J. Katz & al (2010) Applications of holography in fluid mechanics and particle dynamics, *Annual Review of Fluid Mechanics*, **42**, 531–555

[7] L. Méès & al (2013) Evaporating droplet hologram simulation for digital in-line holography setup with divergent beam, *Journal of the Optical Society of America*, **30**, 2021–2028

[8] J.-L. Marié & al (2017) Digital holographic measurement of the lagrangian evaporation rate of droplets dispersing in a homogeneous isotropic turbulence, *Experiments in Fluids*, **58**(2), 11

[9] F. Jolivet & al (2018) Regularized reconstruction of absorbing and phase objects from a single in-line hologram, application to fluid mechanics and micro-biology, *Optics Express* **26**, 8923-8940

[10] S.-H. Lee & al (2007) Characterizing and tracking single colloidal particles with video holographic microscopy, *Optics Express*, **15**(26), 18275–18282

[11] S. Ferréol & al (2007) Inverse problem approach in Particle Digital Holography : out-of-field particle detection made possible, *Journal of the Optical Society of America*, **24** (12), 3708–3716

[12] S. Ferréol & al (2007) Inverse problem approach for particle digital holography: accurate location based on local optimization, *Journal of the Optical Society of America*, **24**(4), 1164–1171

[13] C. Wang, (2016) Holographic characterization of protein aggregates, *Journal of pharmaceutical sciences*, **105**(3), 1074–1085

[14] L. Philips (2017) Holographic characterization of contaminants in water: Differentiation of suspended particles in heterogeneous dispersions, *Water research*, **122**, 431–439
[15] J. W. Goodman (2005) Introduction to Fourier optics, *Roberts*
[16] R. W. Gerchberg and W. O. Saxton, (1972) A practical algorithm for the determination of the phase from image and diffraction plane pictures, *Optik*, **35**, 237–246
[17] J. R. Fienup, (1982) Phase retrieval algorithms: a comparison, *Applied Optics*, **21**, 2758–2769
[18] L. Denis & al (2009) Inline hologram reconstruction with sparsity constraints, *Optics Letters*, **34**, 3475–3477
[19] E. Wolf, Three-dimensional structure determination of semi-transparent objects from holographic data, *Optics Communications*, **1**(4), 153–156
[20] G. Mie (1908) Beiträge zur optik trüber medien, speziell kolloidaler metallösungen, *Annalen der physik*, **330**, 377–445